08 Aug 2014

Thermal Transport Across a Substrate-Thin-Film Interface: Effects of Film Thickness and Surface Roughness

Zhi Liang
Missouri University of Science and Technology, zlch5@mst.edu

Kiran Sasikumar

Pawel Keblinski

Recommended Citation

Z. Liang et al., "Thermal Transport Across a Substrate-Thin-Film Interface: Effects of Film Thickness and Surface Roughness," *Physical Review Letters*, vol. 113, no. 6, article no. 65901, American Physical Society, Aug 2014.
The definitive version is available at https://doi.org/10.1103/PhysRevLett.113.065901

Thermal Transport across a Substrate–Thin-Film Interface: Effects of Film Thickness and Surface Roughness

Zhi Liang,[1,*] Kiran Sasikumar,[2] and Pawel Keblinski[1,2,†]
[1]Rensselaer Nanotechnology Center, Rensselaer Polytechnic Institute, Troy, New York 12180, USA
[2]Department of Materials Science and Engineering, Rensselaer Polytechnic Institute, Troy, New York 12180, USA
(Received 24 December 2013; published 8 August 2014)

Using molecular dynamics simulations and a model AlN-GaN interface, we demonstrate that the interfacial thermal resistance R_K (Kapitza resistance) between a substrate and thin film depends on the thickness of the film and the film surface roughness when the phonon mean free path is larger than film thickness. In particular, when the film (external) surface is atomistically smooth, phonons transmitted from the substrate can travel ballistically in the thin film, be scattered specularly at the surface, and return to the substrate without energy transfer. If the external surface scatters phonons diffusely, which is characteristic of rough surfaces, R_K is independent of film thickness and is the same as R_K that characterizes smooth surfaces in the limit of large film thickness. At interfaces where phonon transmission coefficients are low, the thickness dependence is greatly diminished regardless of the nature of surface scattering. The film thickness dependence of R_K is analogous to the well-known fact of lateral thermal conductivity thickness dependence in thin films. The difference is that phonon-boundary scattering lowers the in-plane thermal transport in thin films, but it facilitates thermal transport from the substrate to the thin film.

DOI: 10.1103/PhysRevLett.113.065901 PACS numbers: 65.40.-b, 63.22.-m, 66.70.-f

Phonon scattering from external interfaces is well known to reduce thermal conductivity as it limits the phonon mean free path (MFP). In particular, recent studies on silicon nanowires with rough surfaces [1] demonstrated a dramatic reduction of the nanowire thermal conductivity, not observed in studies of nanowires with smoother surfaces. Similarly, thin films of submicrometer thickness attached to a bulk substrate, which are widely used in semiconductor and MEMS devices [2–4], can exhibit reduced in-plane thermal conductivity due to phonon-boundary scattering if the thickness of the film is smaller than the bulk phonon MFP [5–7].

However, the thickness dependence of interfacial thermal resistance [8] (Kapitza resistance) R_K at the substrate–thin-film interface and the influence of phonon boundary scattering (scattering at the film outer surface) on R_K are not well understood. In several experiments [9,10], it was found that R_K at an epitaxial Bi thin film–Si substrate interface is essentially independent of film thickness. However, in the recent experiments, it was observed that R_K between two multiwall carbon nanotubes (MWCNTs) strongly depends on the number of walls in each MWCNT [11], which manifests a clear thickness effect on R_K. To elucidate these different behaviors, we present theoretical analysis and results of molecular dynamics simulations on a model substrate–thin-film interface.

The underlying reason for the above-discussed phenomena is illustrated in Fig. 1. When the phonon arrives from the substrate, a fraction of its energy gets transmitted to the film. However, without a thermalizing scattering event (such as phonon-phonon or diffuse interfacial scattering), the phonon can ballistically travel in the thin film and be reflected specularly by the surface, particularly if the surface is atomistically smooth. In this case, the phonon may transmit back to the substrate without any energy transfer to the thin film. This effectively reduces the phonon transmission coefficient and increases the interfacial thermal resistance R_K. Such an effect can be eliminated by a rough outer surface, which scatters most phonons diffusely; i.e., in this case phonons are thermalized at the outer surface.

We first develop a theoretical model to determine quantitatively the effect of the outer surface scattering on the interfacial thermal transport between the substrate and thin film. We label the substrate to be material 1 and thin film to be material 2. The thickness of the substrate and thin film is L_1 and L_2, respectively (see Fig. 1). L_1 is much greater than the phonon MFP of the substrate material.

The Kapitza conductance, G_K $(=1/R_K)$, can be estimated by summation over all phonon contributions using [12–17]

$$G_K = \frac{1}{2}\sum_j \int_0^{\pi/2} \int_0^{\omega_1^{\max}} d\omega \frac{dN_{1,j}(\omega, T)}{dT} \times \hbar\omega v \cos\theta_1 \alpha_{1\to 2}(\theta_1, j, \omega) \sin\theta_1 d\theta_1. \quad (1)$$

In Eq. (1), j is the phonon branch, ω is the phonon frequency, $\omega_1^{\max}$ and $N_{1,j}$ are, respectively, the maximum phonon frequency and the mode-dependent phonon distributions function in the substrate, T is the temperature, $\hbar$ is the Planck constant divided by 2π, v is the phonon group

velocity, θ is the angle between the normal to the interface and the phonon propagation direction, and $\alpha_{1\to2}$ is the phonon transmission coefficient.

For our consideration, we estimate $\alpha_{1\to2}$ from the acoustic mismatch model (AMM) [12]

$$\alpha_{1\to2} = \alpha(\theta_1) = \frac{4z_1 z_2 \cos\theta_1 \cos\theta_2}{(z_1 \cos\theta_1 + z_2 \cos\theta_2)^2}, \tag{2}$$

where $z_1 = \rho_1 v_1$ and $z_2 = \rho_2 v_2$ are the acoustic impedances, ρ's are the densities, and θ_1 and θ_2 are related by Snell's law as $\sin\theta_1/v_1 = \sin\theta_2/v_2$. The above formula for phonon transmission should be applicable to high-quality, epitaxial interfaces over low and intermediate phonon frequencies. For high frequencies, a modification of Eq. (2) is needed to account for the discrete nature of the material, however, we will neglect this detail.

To estimate the effective transmission coefficient α_{eff}, we calculate the total phonon energy returning to the substrate by considering incident phonon with energy E_i arriving at incident angle θ_1. $E_{r,n}$ denotes phonon energy returning to the substrate after traveling back and forth in the thin film n times. The expression for $E_{r,n}$ is given by (see Fig. 1);

$$\begin{aligned} E_{r,0} &= [1-\alpha(\theta_1)]E_i \\ E_{r,1} &= \alpha^2(\theta_1) p e^{-2(L_2/\cos\theta_2)/\lambda_2} E_i \\ E_{r,2} &= \alpha^2(\theta_1) p^2 [1-\alpha(\theta_1)] e^{-4(L_2/\cos\theta_2)/\lambda_2} E_i \\ &\cdots \end{aligned} \tag{3}$$

where p is the specularity of the thin film surface and λ_2 is the phonon MFP of bulk material 2. We considered that the phonon energy is truly transmitted to the film if it either gets scattered within the film with a probability $[1-\exp(-l/\lambda_2)]$, where l is the traveled distance, or it is diffusely scattered at the surface with a probability of $(1-p)$.

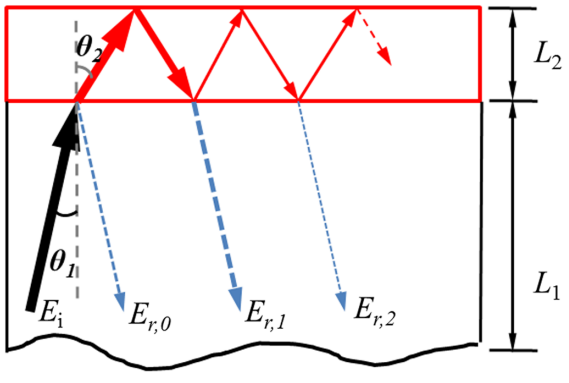

FIG. 1 (color online). Schematic diagram of the model system depicting multiple phonon scattering processes at the substrate–thin-film interface.

Using Eqs. (3), by summing all the reflected energies, we obtain an expression for α_{eff}

$$\begin{aligned} \alpha_{\text{eff}}(\theta_1, L_2) &= 1 - \frac{\sum_n E_{r,n}}{E_i} \\ &= \alpha(\theta_1) \frac{1 - p e^{-2(L_2/\cos\theta_2)/\lambda_2}}{1 - [1-\alpha(\theta_1)] p e^{-2(L_2/\cos\theta_2)/\lambda_2}}. \end{aligned} \tag{4}$$

It is seen from Eq. (4) that (i) α_{eff} is smaller than $\alpha(\theta_1)$ unless $p = 0$ or $L_2 \to \infty$, (ii) α_{eff} is a function of thin film thickness resulting in thickness dependent G_K, (iii) when $p = 0$, which represents a completely diffuse phonon scattering at the surface, is α_{eff} independent of L_2, (iv) when $\alpha(\theta_1) \ll 1$, which is the case for highly dissimilar materials, the thickness dependence is also eliminated. The thickness dependent G_K is determined by replacing $\alpha_{1\to2}$ in Eq. (1) with α_{eff}.

The above analysis is consistent with recent experimental observations by Yang *et al.* [11] on contacts between two MWCNTs with varying diameter and wall thickness. By contrast, Hanisch *et al.* [9] and Krenzer *et al.* [10] observed thickness independent resistance at an epitaxial Bi thin film on Si substrate. In the latter cases, the interfaces are formed by highly dissimilar materials and, thus, are characterized by high interfacial resistance. Consequently, the phonon transmission coefficients at such interfaces are expected to be small [$\alpha(\theta_1) \ll 1$], and according to Eq. (4), in this limit, the thickness dependence is eliminated.

Now we turn into an atomistic model and simulations to examine applicability of the theoretical model. We select GaN as the substrate and AlN as the adlayer. Both materials have a Wurtzite hexagonal crystal structure. The atomic interactions are modeled using the Stillinger-Weber (SW) potential with parameters developed by Bere and Serra (for GaN) [18] and Lei (for AlN) [19]. To be consistent with the potential parameters developed by Lei [19], only the nearest neighbors are considered in our simulation.

MD simulation equilibration runs at 300 K and 1 atm using Berendsen thermostat and barostat [20] predict that the lattice constants are $a = 3.19$ Å, $c = 5.22$ Å for GaN and $a = 3.09$ Å, $c = 5.05$ Å for AlN, which agree well with the experimental data [21]. The phonon group velocity v is predicted from the slope of the phonon frequency (ω) vs wave vector (κ) dispersion curves, which are determined using the harmonic force constants based on the SW potential. We estimate v in each material as the average of the three [0001] acoustic phonon group velocities in the $\kappa \to 0$ limit. Using the calculated lattice constants and phonon group velocities, we obtain the acoustic impedance ratio $z_{\text{GaN}}/z_{\text{AlN}} \approx 1.6$.

To estimate the phonon MFP, we resort to a method proposed by Schelling *et al.* [22]. The method involves calculating the thermal conductivity k of a bulk material

using MD simulations with different simulation box sizes. In the MD model, the $[1\bar{1}00]$, $[11\bar{2}0]$, and [0001] directions of the GaN or AlN crystal are aligned, respectively, in the x, y, and z (see Fig. 2). In the calculation of thermal conductivity, the simulation box only consists of one material at each time. The simulation box has a cross section area of three unit cells in the x direction by five unit cells in the y direction, which has been shown to be large enough to remove the possible size effect [23]. The periodic boundary conditions are applied in the x and y directions. Along the z direction of heat propagation, the length L varies from 38 nm to 150 nm. The simulation box is bordered by a 10-unit-cell long heat source and heat sink regions and free boundaries. Hence, the system has zero stress in the z direction in all cases. A velocity Verlet algorithm with a time step size of 1 fs is used for the integration of equations of motions [24].

The system is first equilibrated at 300 K for 1 ns. After the system reaches thermal equilibrium, the global thermostat is turned off, and a heat flux of 15 GW/m^2 is applied by adding a constant amount of energy to the heat source and removing the same amount of energy from the heat sink at each time step using the velocity rescaling method [25]. Each simulation run is carried out for 6 ns to allow the system to reach a steady state, and then for additional 50 ns for data collection. The thermal conductivity is obtained from Fourier's law. A linear fit of $1/k$ vs $1/L$ predicts $k_1(L \to \infty) \approx 166 \pm 11$ W/m K and $\lambda_1 \approx 52$ nm for GaN. Similarly, we obtain $k_2(L \to \infty) \approx 472 \pm 29$ W/m K and $\lambda_2 \approx 127$ nm for AlN.

Now, we turn our attention to MD simulations of thermal transport across the GaN|AlN interface. To create an epitaxial interface, we strain the cross section of GaN to fit the lattice constants of AlN in the x and y directions. We fix the length of GaN L_1 to 200 unit cells, which is about $2\lambda_1$ in all cases. Additionally, half of the atoms in the region ranging from 0 to 8 nm from the GaN surface are removed to generate a very rough surface as shown in the inset of Fig. 2(a). The rough surface can scatter the majority of phonons reach the GaN surface diffusely thus mimicking a semi-infinite substrate. For AlN thin film, we vary its length L_2 from 13 to 76 nm.

The surface specularity p can be tuned by varying the roughness of the surface [26]. Hence, we consider two types of AlN surfaces. One is an atomically smooth surface that scatters almost all phonons specularly, corresponding to $p \approx 1$. In another case, we generate a very rough AlN surface as we did at the GaN surface where most phonons scatter diffusely, corresponding to $p \approx 0$. To remove the artificial mechanical stresses present in an as prepared heterogeneous system, we performed energy minimization before MD simulations. Also, we imposed lower heat flux of 5 GW/m^2 to limit temperature drop ΔT at the interface.

Typical temperature profiles in the case of $L_2 \approx 20$ nm are shown in Fig. 2. The Kapitza resistance is determined by $R_K = \Delta T/q$. It is evident from Fig. 2 that ΔT at the interface involving a rough surface is much lower than that involving a smooth surface.

In Fig. 3, we show R_K obtained in MD simulations vs the inverse of the film thickness. In the case of a rough external surface, R_K is around 0.77 m^2 K/GW and is essentially independent of film thickness. This is consistent with our model assuming $p = 0$, i.e., fully diffusive surface scattering. In this case, α_{eff} and R_K are L_2 independent.

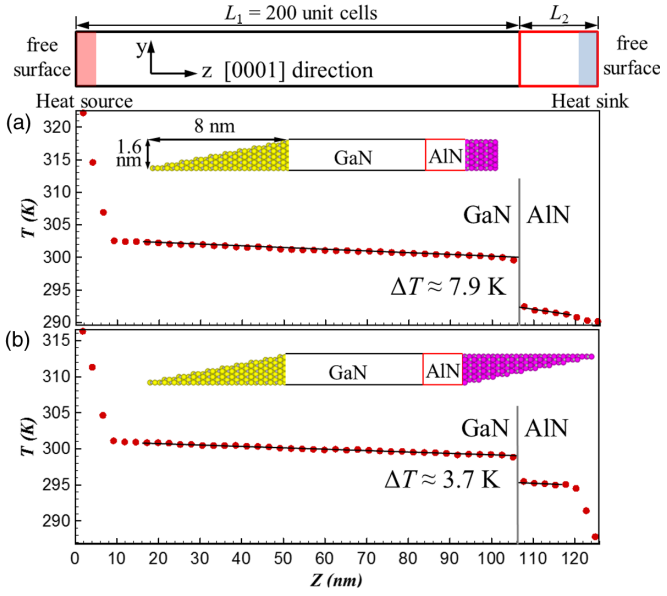

FIG. 2 (color online). Schematic diagram of the simulation box and the corresponding temperature profiles in NEMD simulation. (a) Smooth and (b) rough external AlN surface.

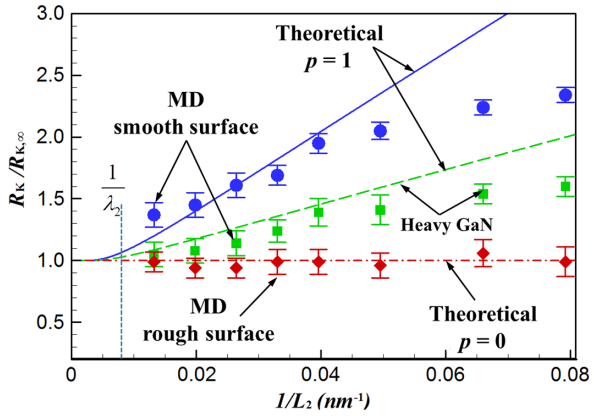

FIG. 3 (color online). MD simulation results and theoretical prediction of R_K as a function of L_2, normalized by R_K for $L_2 \to \infty$. The horizontal dash dot shows a size-independent R_K model prediction for diffusive surface ($p = 0$). The solid and dashed lines show prediction for specular surface ($p = 1$) in the case of GaN|AlN structure and heavy-GaN|AlN structure, respectively. The vertical dashed line indicates phonon MFP (λ_2). The uncertainties are determined from the analysis of six independent simulation runs.

In the case of a smooth surface, R_K shows clear thickness dependence. As shown in Fig. 3, MD simulation results have a good agreement with the theoretical prediction for a perfectly specular surface ($p = 1$) for L_2 greater than 25 nm. The discrepancy with the theoretical model predictions for smaller film thicknesses might be due to the fact that the acoustic phonons with long MFPs have very small contributions to the interfacial thermal transport because they have a very low possibility of thermalizing in the thin film or at the smooth surface. Therefore, short-MFP phonons including optical phonons may dominate the interfacial thermal transport and it might not be appropriate to use a single MFP and single specularity parameter approximation in theoretical considerations.

To demonstrate broad validity of our theoretical model, we artificially increased the mass and interaction strength in GaN by a factor of 5 such that the acoustic impedance ratio increases to eight, while frequencies remain unchanged. With a rough external surface, we find R_K at the heavy-GaN|AlN interface is around 12.0 m^2 K/GW and is essentially independent of film thickness. With a smooth external surface, it is shown in Fig. 3 that the size effect is much smaller compared to that at original GaN|AlN interface, due to lower value of α. The result is again consistent with our theoretical prediction. Furthermore, we also observe analogous size effects when AlN is the substrate and GaN is the adlayer (see Supplemental Material [27]).

To this extent, we performed phonon localization analysis [28–30] (details are described in Supplemental Material [27]), which demonstrates that for smooth external surfaces, a limited number of high frequency modes are localized at the surface. Phonon-phonon scattering with these surface modes may be substantial for high-frequency phonons thus leading to more diffuse surface scattering. In the case of the rough surfaces, we observed a number of localized low-frequency surface modes. These may be a contributor to diffuse scattering across the whole frequency range consistent with our simulation results. Our analysis also demonstrated the presence of a few low- and high-frequency modes localized at the epitaxial interface. These modes might lead to frequency dependent $\alpha_{1\to2}$ for phonons with similar frequency, but due to their limited number should be rather inconsequential for the overall interfacial resistance.

We also notice that there were a number of studies where the roughness was introduced to interfaces to improve interfacial conductance [31,32], in particular when there is a large acoustic mismatch leading to a significant diffuse scattering at interfaces, rather than at external surfaces. The detailed analysis of such systems, where both internal interface and external surfaces may exhibit a combination of diffuse and specular or acoustic scattering requires separate work. However, we expect smaller size effects on thermal transport across rough interfaces, as the size effects are maximized when $\alpha_{1\to2}$ is very high (close to unity in our model). By contrast, diffuse interfacial scattering is characterized by $\alpha_{1\to2}$ in the 50% range [31,32].

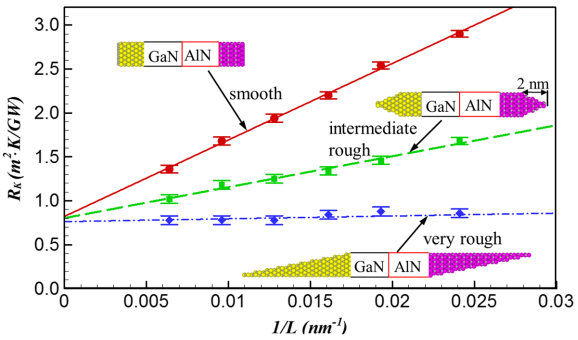

FIG. 4 (color online). MD simulation results of R_K as a function of total length L of the GaN|AlN structure. The lines are linear fits to the R_K vs $1/L$ for structures with different surface roughness. The uncertainties are determined from the analysis of four independent simulation runs.

To determine the R_K of an isolated interface using MD simulations, a standard practice is to gradually increase the length of two leads until there is no significant size effect on R_K. Our theoretical analysis and the results of MD simulations show that with rough external surfaces, one can determine interfacial thermal conductance with relatively small system sizes. To this end, we studied GaN|AlN epitaxial interface with the GaN lead and AlN lead that contain the same number of unit cells in the heat flow direction. The total length L of the structure is varied from 40 to 150 nm. As shown in Fig. 4, three types of surface roughness are considered in the MD model, (i) smooth surfaces, (ii) moderately rough surfaces, and (iii) very rough surfaces.

In the case of smooth surfaces, R_K exhibits a strong size dependence. A moderately rough surface diminishes the magnitude of the size effect and leads to the same extrapolated value when $L \to \infty$. However, in both cases, a series of simulations are required with a simulations box length as large as phonon MFP to determine the asymptotic R_K corresponding to the characteristics of an isolated interface. Similar size effects on R_K were observed by others [17,33,34]. By extrapolating R_K to an infinite system length limit, the system with smooth surface and moderately rough surfaces predicts $R_{K,\infty} \approx 0.82$ m^2 K/GW.

By contrast, R_K is essentially size independent if very rough external surfaces are used. In this case, a linear fit of R_K vs $1/L$ gives an almost horizontal line and predicts $R_{K,\infty} \approx 0.77$ m^2 K/GW. In this case, the simulation results with system sizes as small as 40 nm, i.e., several times smaller than MFP, yield a size-converged value.

Our simulation results indicate that the phonon-boundary scattering strongly depends on the magnitude of the surface roughness, and also on the phonon wavelength. At moderately rough surfaces, short-wavelength phonons scatter diffusely, but long-wavelength phonons

scatter specularly. This behavior was also considered in the explanation of phonon transport through semiconductor nanowires that were surrounded by amorphous oxide shells [1,35,36]. In particular, to explain the unusual linear temperature dependence of nanowire thermal conductivity at low temperatures, Chen *et al.* [1] assumed specular boundary scattering of long-wavelength phonons and diffuse scattering of short-wavelength phonons, which is analogous to our observations.

In summary, we use a theoretical model and MD simulations to investigate the size effect on the R_K of a substrate–thin-film interface. We find that if the phonons transmitted from a substrate are not scattered diffusely in the material or at the surface, they can return to the substrate and reduce the effective phonon transmission coefficient. The size effect on R_K is a combined effect of internal and boundary scattering. Introducing very rough surfaces results in a size-independent R_K. This result is also useful in calculation of the R_K of an isolated interface.

This work is supported by ARL research center: Alliance for the Computationally Guided Design of Energy Efficient Electronic Materials and by the NY State NYSTAR funded Focus Interconnect Center. We would like to thank the National Institute for Computational Science (NICS) for providing us supercomputer resources for MD simulations.

*liangz3@rpi.edu
†keplip@rpi.edu

[1] R. Chen, A. I. Hochbaum, P. Murphy, J. Moore, P. Yang, and A. Majumdar, Phys. Rev. Lett. **101**, 105501 (2008).
[2] A. M. Marconnet, M. Asheghi, and K. E. Goodson, J. Heat Transfer **135**, 061601 (2013).
[3] B.-Y. Nguyen, G. Celler, and C. Mazure, J. Integr. Circuit Syst. **4**, 51 (2009).
[4] M. Lutz, A. Partridge, P. Gupta, N. Buchan, E. Klaassen, J. McDonald, and K. Petersen, in *14th International Conference on Solid-State Sensors, Actuators and Microsystems Conference* (IEEE, Lyon, France, 2007), p. 49.
[5] A. D. McConnell and K. E. Goodson, Annual review of heat transfer **14**, 129 (2005).
[6] D. G. Cahill, W. K. Ford, K. E. Goodson, G. D. Mahan, A. Majumda, H. J. Maris, R. Merlin, and S. R. Phillpot, J. Appl. Phys. **93**, 793 (2003).
[7] W. Liu and M. Asheghi, Appl. Phys. Lett. **84**, 3819 (2004).
[8] P. L. Kapitza, J. Phys. (Moscow) **4**, 181 (1941).
[9] A. Hanisch, B. Krenzer, T. Pelka, S. Mollenbeck, and M. Horn-von Hoegen, Phys. Rev. B **77**, 125410 (2008).
[10] B. Krenzer, A. Hanisch-Blicharski, P. Schneider, T. Payer, S. Mollenbeck, O. Osmani, M. Kammler, R. Meyer, and M. Horn-von Hoegen, Phys. Rev. B **80**, 024307 (2009).
[11] J. Yang, M. Shen, Y. Yang, W. J. Evans, Z. Wei, W. Chen, A. A. Zinn, Y. Chen, R. Prasher, T. T. Xu, P. Keblinski, and D. Li, Phys. Rev. Lett. **112**, 205901 (2014).
[12] E. T. Swartz and R. O. Pohl, Rev. Mod. Phys. **61**, 605 (1989).
[13] P. Reddy, K. Castelino, and A. Majumdar, Appl. Phys. Lett. **87**, 211908 (2005).
[14] C. Kimmer, S. Aubry, A. Skye, and P. K. Schelling, Phys. Rev. B **75**, 144105 (2007).
[15] H. Zhao and J. B. Freund, J. Appl. Phys. **97**, 024903 (2005).
[16] M. Shen, P. K. Schelling, and P. Keblinski, Phys. Rev. B **88**, 045444 (2013).
[17] E. S. Landry and A. J. H. McGaughey, Phys. Rev. B **80**, 165304 (2009).
[18] A. Bere and A. Serra, Phys. Rev. B **65**, 205323 (2002).
[19] H. P. Lei, Ph.D. thesis, Caen University, 2009.
[20] H. J. C. Berendsen, J. P. M. Postma, W. F. Van Gunsteren, A. Di Nola, and J. R. Haak, J. Chem. Phys. **81**, 3684 (1984).
[21] W. Qian, M. Skowronski, and G. R. Rohrer, in *Material Research Society Symposium Proceedings* 423, 475 (1996).
[22] P. K. Schelling, S. R. Phillpot, and P. Keblinski, Phys. Rev. B **65**, 144306 (2002).
[23] X. W. Zhou, S. Aubry, R. E. Jones, A. Greenstein, and P. K. Schelling, Phys. Rev. B **79**, 115201 (2009).
[24] D. Frenkel and B. Smit, *Understanding Molecular Simulation* (Academic Press, San Diego, 2002), p. 75.
[25] P. Jund and R. Jullien, Phys. Rev. B **59**, 13707 (1999).
[26] S. B. Soffer, J. Appl. Phys. **38**, 1710 (1967).
[27] See Supplemental Material at http://link.aps.org/supplemental/10.1103/PhysRevLett.113.065901 which includes Refs. [28–30] for Results of Rk at the interface between the GaN adlayer and AlN substrate, and phonon localization analysis.
[28] L. T. Kong, Comput. Phys. Commun. **182**, 2201 (2011).
[29] A. Bodapati, P. K. Schelling, S. R. Phillpot, and P. Keblinski, Phys. Rev. B **74**, 245207 (2006).
[30] C. Campañá and M. H. Müser, Phys. Rev. B **74**, 075420 (2006).
[31] X. W. Zhou, R. E. Jones, C. J. Kimmer, J. C. Duda, and P. E. Hopkins, Phys. Rev. B **87**, 094303 (2013).
[32] R. J. Stevens, L. V. Zhigilei, and P. M. Norris, Int. J. Heat Mass Transfer **50**, 3977 (2007).
[33] R. E. Jones, J. C. Duda, X. W. Zhou, C. J. Kimmer, and P. E. Hopkins, Appl. Phys. Lett. **102**, 183119 (2013).
[34] T. Watanabe, B. Ni, S. R. Phillpot, P. K. Schelling, and P. Keblinski, J. Appl. Phys. **102**, 063503 (2007).
[35] A. I. Hochbaum, R. Chen, R. D. Delgado, W. Liang, E. C. Garnett, M. Najarian, A. Majumdar, and P. Yang, Nature (London) **451**, 163 (2008).
[36] N. Mingo and L. Yang, Phys. Rev. B **68**, 245406 (2003).